Available online at www.eccomasproceedia.org
Eccomas Proceedia COMPDYN (2023) 2017-2037

ECCOMAS
Proceedia

COMPDYN 2023
9th ECCOMAS Thematic Conference on
Computational Methods in Structural Dynamics and Earthquake Engineering
M. Papadrakakis, M. Fragiadakis (eds.)
Athens, Greece, 12-14 June 2023

SIMPLIFIED-MICRO MODELLING OF UNREINFORCED AND JOINT REPOINTED BRICK MASONRY

Maja Gosheva[1], Sergey Churilov[2], Elena Dumova-Jovanoska[2], Veronika Shendova[1], and Lidija Krstevska[1]

[1] Ss. Cyril and Methodius University in Skopje, Institute of Earthquake Engineering and Engineering Seismology
Todor Aleksandrov 165, P.O. Box 101, 1000 Skopje, N. Macedonia
maja.gosheva@gmail.com, {veronika, lidija}@iziis.ukim.edu.mk

[2] Ss. Cyril and Methodius University in Skopje, Faculty of Civil Engineering
Blvd. Partizanski odredi 24, P.O. Box 560, 1000 Skopje, N. Macedonia
{curilov, dumova}@gf.ukim.edu.mk

Abstract

The need to strengthen old masonry structures in seismic regions is required in order to meet the requirements of more sophisticated codes and regulations. Masonry as a building material exhibits highly nonlinear behaviour, which makes analytical calculations of these structures for the purpose of strengthening them extremely difficult. In order to simplify the analysis, a finite element model using simplified-micro (meso) modelling strategy has been adopted. Concrete damage plasticity model (CDP) was used for homogenization of the bricks and mortar joints. Cohesive surface-based behaviour (interface elements) was used for modelling the discontinuity in the "homogenous" material, simulating the cracks in the joints and the middle of the bricks through the traction–separation behaviour of the cohesive element. For verification of the modeming assumptions, a set of experimental tests of the masonry components and masonry assemblages were carried out. In this study, unreinforced and strengthened masonry wallets were tested under compression and diagonal tension (shear) loads. The strengthening of the masonry was performed by repointing the mortar joints with polymer-cement mix with added polypropylene fibres. In addition, polypropylene straps were inserted into the horizontal joints. The simulation results are in good agreement with the experimental behaviour of the masonry assemblages, indicating promising results for strengthening the masonry.

Keywords: Earthquake Engineering, Masonry, Strengthening, Repointing, Experimental Tests, Simplified Micro-Modelling, Concrete Damage Plasticity.

ISSN:2623-3347
Peer-review under responsibility of the organizing committee of COMPDYN 2023.
doi: 10.7712/120123.10539.21042

1 INTRODUCTION

Masonry represents the start of the building history due to its simplicity in laying pieces of stone or man-made bricks, one on top of another, bonded together with or without adhesive material. Apart from its simplicity, masonry has many advantages like low maintenance, durability, good fire protection, sound absorption and aesthetics, which made it the most used building material throughout the years. These, now old masonry structures, were made based on the expert masons' experience acquired through trial and errors, without complicated calculations and analysis, which is contrary to the new sophisticated, more accurate and predictable design methods [1]. As a result of that, there is limited amount of knowledge for the bearing capacity of these structures, which further complicates the matter in regions with high seismic excitations. Over time, due to the low ductility and tensile strength, many masonry structures have collapsed and caused great damages, lot of casualties and has razed whole cities to the ground.

Today, with the development of the technology and its application in civil engineering, development of new materials, methods for analysis, codes and regulations there are novel approaches at our disposal. There are methods to strengthen the existing old masonry structures, bring them up to code, and predict their behaviour with numerical simulations for the maximum expected earthquake. Not only we can improve the quality and safety of the existing buildings, but we can also use these resources for additional experimental analysis for new innovative applications of structural masonry in the everyday construction. [1-4]

Masonry strengthening intended to improve the seismic behaviour of a structure is a complex procedure and it can be achieved either by strengthening individual elements or strengthening the structure as a whole [5]. The decision of the strengthening technique depends on the type of masonry itself, on the desired load-bearing capacity, the condition of the structure, as well as the historical significance of the building [4].

Old masonry buildings usually require a complete strengthening of the structural system, which will ensure monolithic behaviour of all structural elements. Most commonly used technics of this type are: strengthening or replacement of the floor slabs, construction of new load-bearing elements, framing the walls, metal bracing and etc. Unlike old traditional masonry structures, newer masonry structures possess a higher degree of seismic resistance due to the connection of the masonry elements with reinforced concrete beams, columns and slabs. In these types of structures strengthening can be applied just on specific, weaker, parts of the structure, like: jacketing, rebuilding a wall, crack injection or joint repointing with mortar with higher strength [5].

Even though every strengthening technique has its pros and cons, after careful consideration of all factors, for this purpose the joint repointing method is chosen as the most suitable, because for its easy and fast application, no need for highly qualified labour, it doesn't change the structural system, which is especially important for buildings with historical and religious significance [3, 4]. Apart from join repointing method and using special mortar with higher strength and ductility, this investigation accounts for inserting polypropylene straps in the horizontal joints. The intention is to further increase the ductility of the masonry when exposed to horizontal loads. These straps are cheap, accessible and easily applicable in the freshly repointed mortar.

2 EXPERIMENTAL PROGRAM

This paper focuses on the numerical simulations of old masonry in both before and after strengthening. The applied strengthening method was joint repointing with a special polymer-cement mix with added polypropylene fibres and polypropylene (PP) straps. The work pre-

sented here is part of a national research project "Masonry strengthening by joint re-pointing – STREP" [3]. To improve the ductility of the masonry, polypropylene straps were inserted into the horizontal joints of the tested assemblages. The straps were 0.7 mm thick and 16 mm wide and they have rough surface texture on both sides for better adhesion. The masonry wallets tested were assembled from solid clay bricks with length of 250 mm, width of 120 mm and height of 60 mm. The mortar quality was compiled so as to simulates old masonry, and was prepared as a combination of pure lime and sand with ratio of 1:3, without addition of any cement com-ponents. This mixture intents to better represent the real state of the existing masonry structures, where this method of strengthening would be applied to.

In order to create a model relevant to the existing masonry in this region, experimental tests were needed to determine the properties of the constitutive materials and the masonry as a structural material. Based on these tests, a numerical model was calibrated and later verified for further application. Tables 1-4 present the basic physical and mechanical properties of the masonry constitutive materials obtained from the tests [4] while the properties of the PP straps were taken from the manufacturer's data.

Bricks	
Type	solid
Material	clay
Dimensions	250 x 120 x 60 mm
Density	2002 kgm^3
Compressive strength	10.64 MPa
Flexural strength	3.04 MPa

Table 1. Physical and mechanical properties of bricks.

Old mortar	
Type	lime
Ratio	1:3
Layer height	10 mm
Density	1650 kgm^3
Compressive strength	0.94 MPa
Flexural strength	0.73 MPa

Table 2. Physical and mechanical properties of old mortar.

Joint repointing mortar	
Type	polymer-cement mix with polypropylene fibres
Depth of repointing of the wall thickness	1:3 on each side of the wall
Compressive strength	32.86 MPa
Flexural strength	12.00 MPa

Table 3. Physical and mechanical properties of join repointing mortar.

Polypropylene straps	
Texture	rough on both sides
Dimensions	16.0 x 0.7 mm
Density	8.06 g/m'
Failure force	1716 – 2353 N
Strain	12 – 14 %

Table 4. Physical and mechanical properties of polypropylene straps.

With the above-mentioned materials, 4 types of assemblages were constructed and experimental tests on the masonry wallets were performed to determinate the compressive and diagonal compressive strength:

I. Masonry subjected to uniaxial compression, Figure 1:
   1. Old unreinforced masonry subjected to uniaxial compression (W – AP)
   2. Strengthened masonry subjected to uniaxial compression (W – AP – RPP)

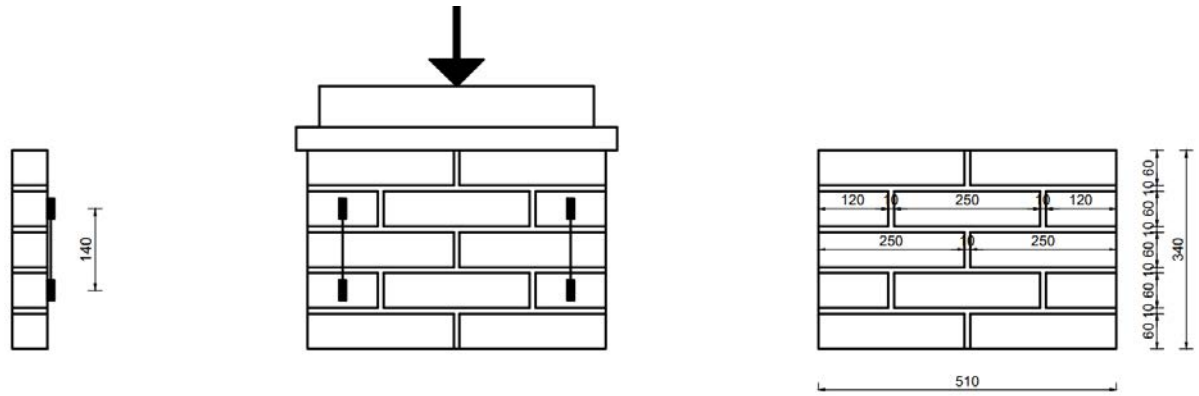

Figure 1. Test set-up for uniaxial compression tests according to EN 1052-1:1999 [6].

II. Masonry subjected to diagonal compression, Figure 2:
   3. Old unreinforced masonry subjected to diagonal compression (W – DP)
   4. Strengthen masonry subjected to diagonal compression (W – DP – RPP)

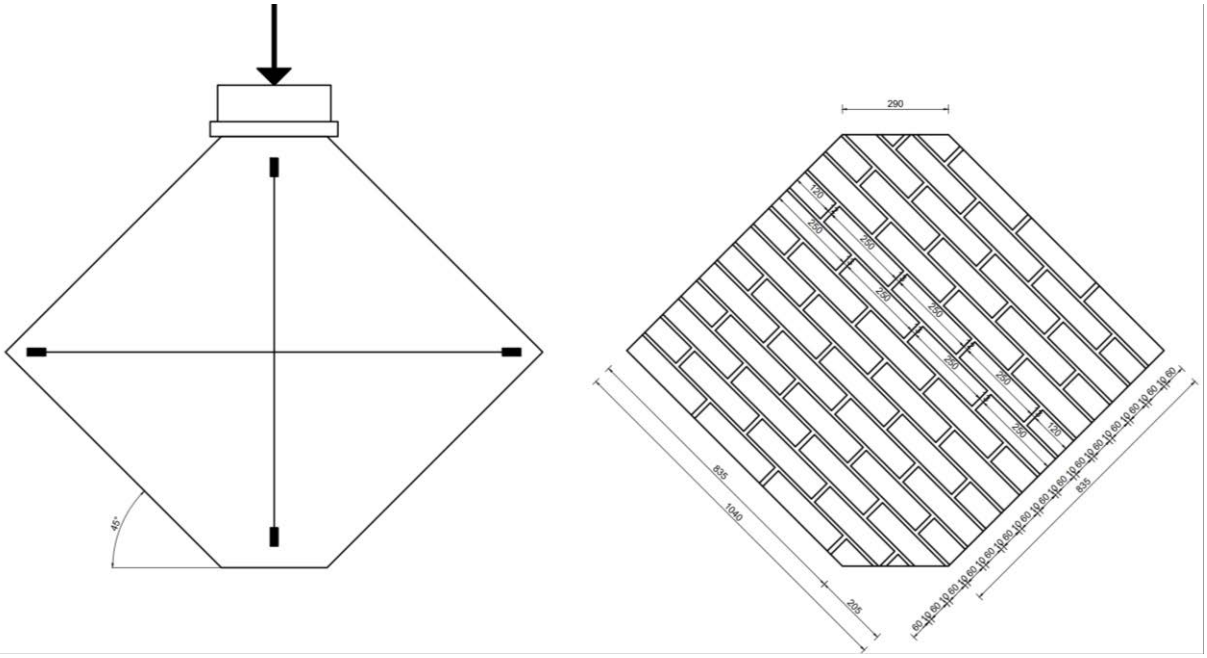

Figure 2. Test set-up for diagonal compression tests according to ASTM E519 – 02 [7].

	Uniaxial compression	Diagonal compression
Old unreinforced masonry	W – AP	W – DP
Strengthened masonry	W – AP – RPP	W – DP – RPP

Table 5. Summarization of the experimental tests with their given abbreviations.

3 RESULTS FROM EXPERIMENTAL TESTS

Three tests were done for each of the four different masonry wallets. The results are shown in Figure 3-6 in a form of force – displacement curves. From the three tests, an average curve has been calculated and later calibration of the calculation model was performed following the average test values.

As for the significance of the results, the strengthened wallets subjected to axial pressure show evident increase in compressive strength of about 20% in comparison to the unreinforced wallets, and about 75% increase in ductility. The strengthened wallets subjected to diagonal compression, present apparent increase in the diagonal compressive (shear) strength of about 67% when compared to the performance of the unreinforced wallets. This is found to be crucial for proper behaviour of masonry buildings in seismic regions and extremely promising for future strengthening of masonry buildings. With respect to the failure mechanisms, the wallets performed as expected by vertical cracking of bricks and vertical joints, for the cases of uniaxial compression and diagonal, stair-case failure for the cases of diagonal compression tests. More details about the tests results can be found in Dumova-Jovanoska et al. [3].

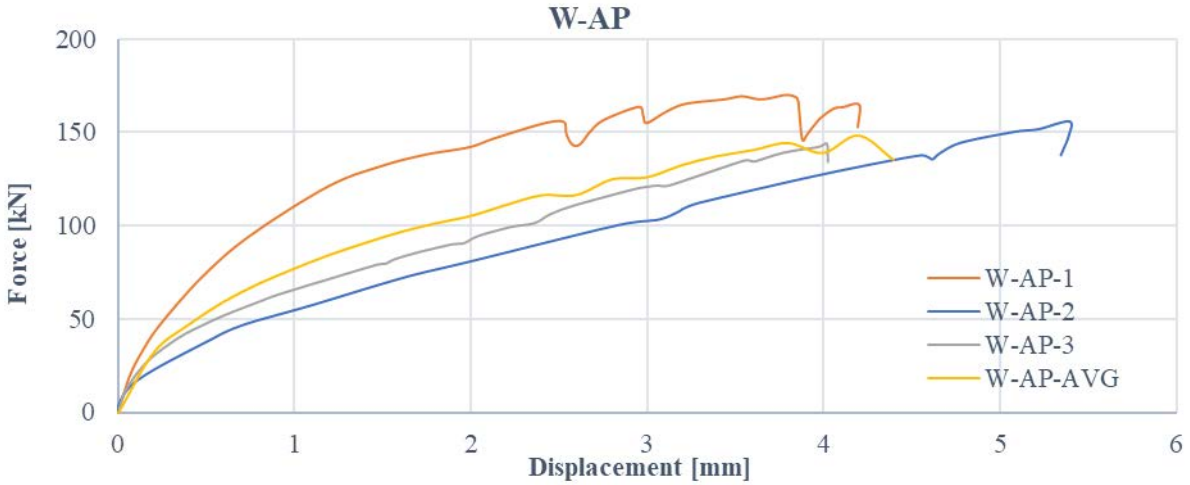

Figure 3. Experimental force-displacement curves for old unreinforced masonry wallets subjected to uniaxial compression.

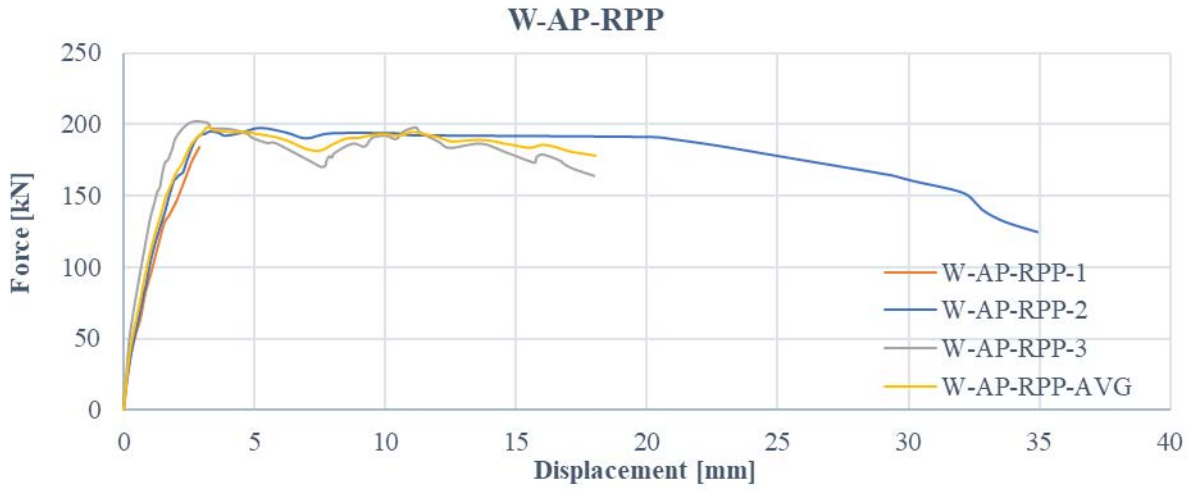

Figure 4. Experimental force-displacement curves for strengthened masonry wallets subjected to uniaxial compression.

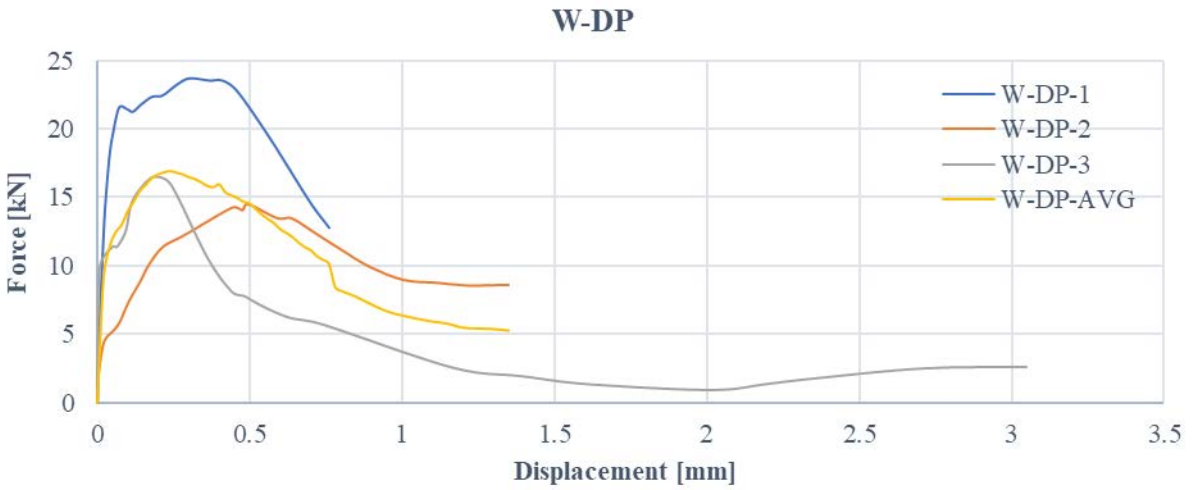

Figure 5. Experimental force-displacement curves for of old unreinforced masonry wallets subjected to diagonal compression.

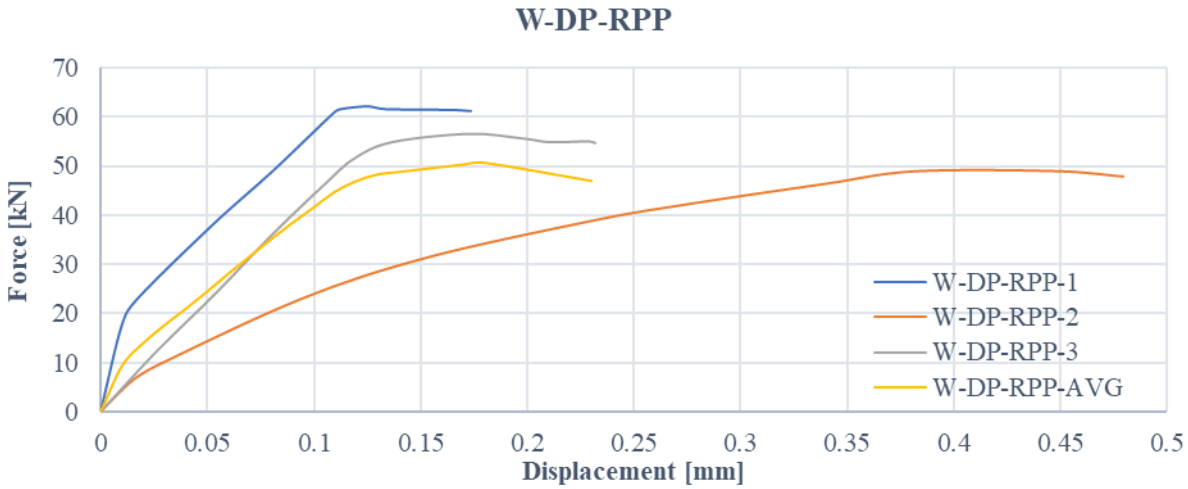

Figure 6. Experimental testing of strengthened masonry wallets subjected to diagonal compression.

4 FINITE ELEMENT MODELING

Foremost, the first decision before modelling is deciding the most convenient modelling method for simulation. Based on an extensive literature review, the authors have found that the most suitable modelling strategy for masonry in this case is the simplified micro-modelling [1, 8-10]. This type of modelling provides results with almost the same accuracy as the micro modelling approach, but in quite easier manner and by using less time for modelling and analysis. Even though macro models, which incorporate homogenization of the masonry as one single material, are even easier to be applied, the results are only approximate and cannot properly predict the local behaviour and failure of masonry. This modelling strategy can be used only for design analysis or large-scale modelling, due to the time efficiency of the analysis [1, 8, 9].

In simplified micro-modelling, it is assumed that the bricks are continuous and mortar joints are presented as interface (connecting) elements between the bricks. Therefore, the bricks are expanded by half of the mortar joint thicknesses, while the mortar joints are simulated by interaction properties that connect the bricks. Figures 7-9 show the dimensions of the test assemblies of the wallets (on the left side) and their simplified micro-models subjected to uniaxial (Figure 7 and 8) and diagonal compression (Figure 9) on the right side.

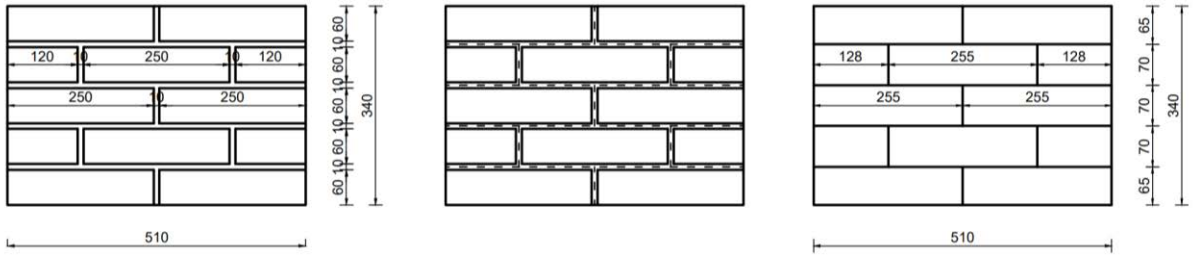

Figure 7. Simplified micro-modelling of masonry wallet subjected to uniaxial compression.

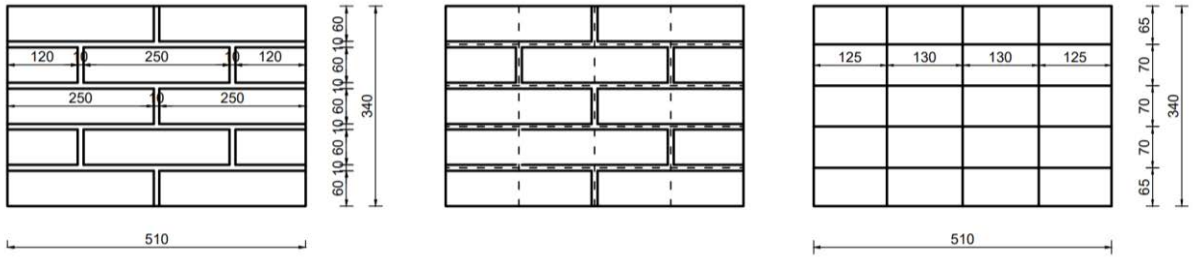

Figure 8. Simplified micro-modelling of masonry wallets subjected to uniaxial compression taking into account possible cracks in the middle of the bricks.

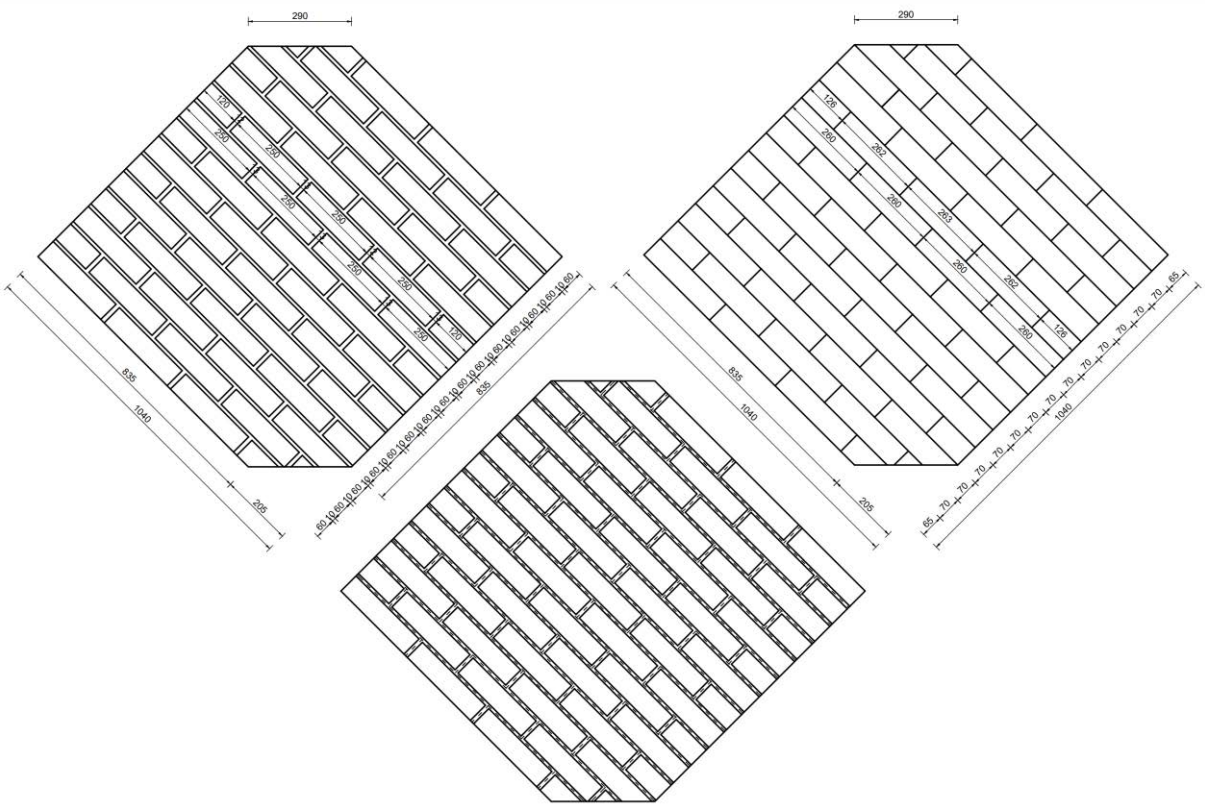

Figure 9. Simplified micro-modelling of masonry wallets subjected to diagonal compression.

With respect to the numerical method for simulation, the analysis can be either implicit or explicit [8]. When performing a nonlinear analysis, the solution cannot be calculated just by solving a single system of equations, as it is done with the linear analyses. Therefore, the increasing load is divided into a certain number of increments and at the end of each increment, the response of the model is calculated. If equilibrium is not achieved during the first iteration

for a given increment, the calculation is repeated with modified stiffness matrix. It often takes several iterations for a given increment to accurately calculate the model's response. This method combines incremental and iterative procedures for solving nonlinear problems [11].

Unfortunately, for highly nonlinear problems such as masonry, an implicit FEM solution often encounters convergence issues and causes analysis termination as the model enters the nonlinear domain. In this case, explicit method should be used to resolve the convergence problems [8]. In this way, the solution is obtained by solving the dynamic equation for each increment with direct progression of the kinematic state from the end of the previous increment, without repetitions of the increment. Explicitly solving the problem does not require the formation of a tangent stiffness matrix, simulations usually require a large number of increments, but since only one equilibrium equation is solved in each increment, the cost per increment is much lower than the one applied in the implicit method [11]. It should be noted that there are also some disadvantages of the explicit analysis, like risk of bad convergence due to the enforced equilibrium and the dependence of the results on the selected time steps [8, 12].

In the investigated cases, the walls subjected to axial compression were calculated with static, implicit analysis due to the simplicity of the models, whereas the analysis of the walls subjected to diagonal compression was computed by using dynamic, explicit analysis, because of convergence problems caused by the highly nonlinear behaviour of the interface elements exposed to shear forces.

The FEM models presented in this paper were simulated in Abaqus Unified FEA software using solid 3-dimensional, 8 node elements with reduced integration (C3D8R) [12]. An element with reduced integration, i.e., only with one integration point located in the middle of the element, was used to overcome the problem of shear locking. This problem occurs in finite element analysis due to the linear nature of the quadrilateral elements, because they cannot accurately model the curvature of the material during bending and therefore additional shear stress appears in the model. Those extra stresses, which otherwise are not real, cause the element to reach equilibrium at smaller displacements, thereby making the element appear stiffer than it actually is. Additionally, since these elements have only one integration point, it is possible to deform them in such a way that the calculated dilations at the integration point will be zero. To avoid this effect, it is necessary to use hourglass control, pay attention to the size of the mesh and avoid loads or boundary conditions in one node, in order to have more reliable results [12].

For best results in terms of reliability of the response and the time required for analysis, finite element mesh size of 20 mm was chosen for the wallets subjected to uniaxial compression and 40 mm for the walls subjected to diagonal compression. The size difference of the meshes comes as a result of the different sizes of the models subjected to uniaxial compression versus diagonal compression. In other words, a smaller model requires a denser mesh and vice versa.

As for the boundary conditions, pinned supports were modelled on the entire bottom surface of the walls. Apart from the wall supports and in order to obtain the descending part of the stress – strain curves, the load subjected to the walls was also modelled through the boundary conditions as a controlled displacement. The applied displacement was taken the same as in the experimental tests of the masonry assemblages and it is shown in the table 6.

Wall	W – AP	W – AP – RPP	W – DP	W – DP – RPP
U2	- 5.0 mm	- 18.0 mm	- 1.5 mm	- 0.5 mm

Table 6. Controlled displacement applied to the top surfaces of the models.

5 CONSTITUTIVE MODELS

5.1 Concrete damaged plasticity model

The bricks in the FE model were represented by the Concrete damaged plasticity (CDP) model. This model has the ability to simulate highly nonlinear behaviour of brittle materials under low confining pressure. It was proposed by Lubliner et. all [13] for concrete with little to no reinforcement. Later, Lee and Fenves [14] further improved the model with modifications to account for the different evolutions of strength under tension and compression. This model enables simulation of irreversible damage and the main failure modes of this model are crushing of the material in compression and cracking in tension [12], Figure 10. These characteristics make the Concrete damaged plasticity model ideal for simulation of masonry as well.

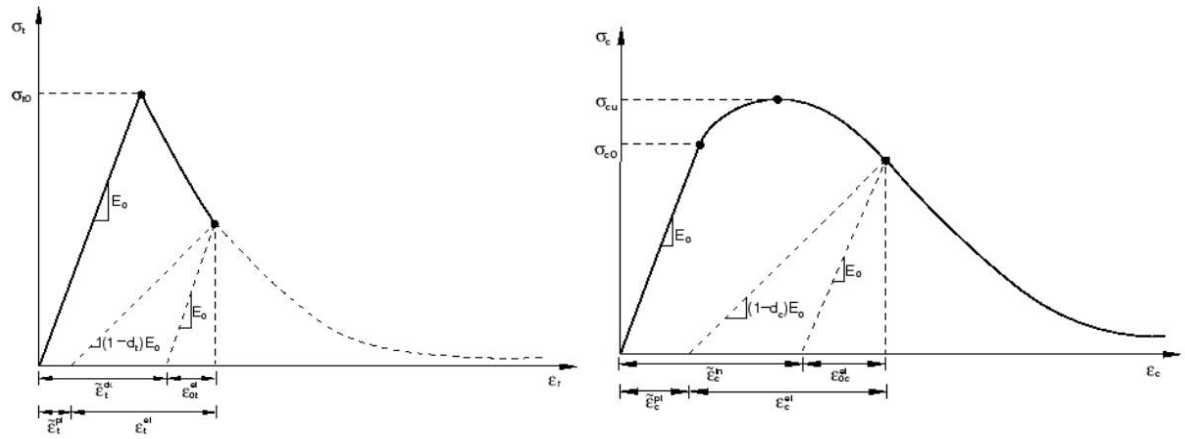

Figure 10. Response of the constitutive model of concrete to uniaxial loading in tension and compression [12].

5.2 Kent and Park model for concrete

The values for the stress – strain curve, required to describe the behaviour of the material, that are necessary for the Concrete Damaged Plasticity model, were calibrated in the FE analysis by using the proposed model from Kent and Park [15]. This model was developed for the purposes of defining the concrete behaviour, either confined or unconfined, Figure 11. In the case of masonry, after excessive comparison, it was noted that the ratio of stress and strain of unconfined concrete corresponds well to the stress – strain ratio of masonry, which makes this model suitable for simulating the true performance of masonry.

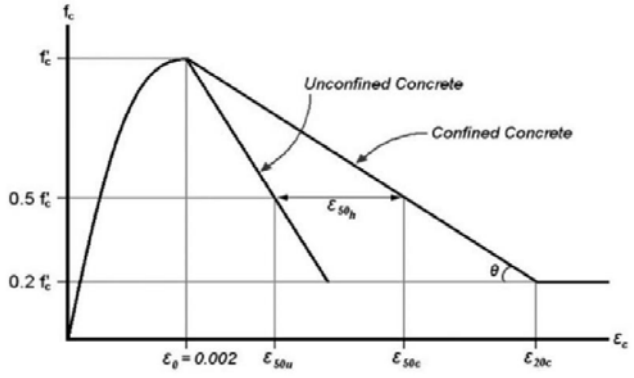

Figure 11. Proposed stress - strain model for unconfined and confined concrete [15].

5.3 Calibration of the FE models

The modulus of elasticity was calculated from the experimentally obtained force – displacement curves [2]. The elastic properties of the used materials are presented in Table 7.

Model	E [MPa]	ν
W – AP	2000	0.15
W – AP – RPP	2000	0.15
W – DP	8000	0.15
W – DP – RPP	15000	0.15

Table 7. Elastic properties of the bricks.

The maximum compressive strength used in Kent and Park's model for calibrating the stress – strain curve was taken from the experimental tests on the wallets subjected to uniaxial compression [2]. The calibration consists of strain adjustments of the curve form the Kent and Park's model to correspond to the maximum strains obtained with the experimental tests.

The tensile strength of the walls was calculated as 1⁄10 of their compressive strength, according to the recommendations of the CDP model [12].

Tables 9 and 10 show the values of the calibrated properties for simulation of the old, unrein-forced and strengthened masonry, accordingly [2].

W – AP		
$\boldsymbol{\sigma_c}$ [MPa]	$\tilde{\varepsilon}_c^{in}$	d_c
0.399	0	0
0.756	0.00175	0
1.071	0.0035	0
1.344	0.00525	0
1.575	0.007	0
1.764	0.00875	0
1.911	0.0105	0
2.016	0.01225	0
2.079	0.014	0
2.100	0.01575	0
2.079	0.0175	0.01
2.016	0.01925	0.04
1.911	0.021	0.09
1.764	0.02275	0.16
1.575	0.0245	0.25
1.344	0.02625	0.36
1.071	0.028	0.49
0.756	0.02975	0.64
$\boldsymbol{\sigma_t}$ [MPa]	$\tilde{\varepsilon}_t^{ck}$	d_t
0.21	0	0
0.0021	0.000945	0.99

Table 8. Calibrated material properties for CPD model for old, unreinforced masonry.

W – AP – RPP		
σ_c [MPa]	$\tilde{\varepsilon}_c^{in}$	d_c
0.494	0	0
0.936	0.00125	0
1.326	0.0025	0
1.664	0.00375	0
1.950	0.005	0
2.184	0.00625	0
2.366	0.0075	0
2.496	0.00875	0
2.574	0.01	0
2.600	0.01125	0
2.574	0.0125	0.01
2.496	0.01375	0.04
2.366	0.015	0.09
σ_t [MPa]	$\tilde{\varepsilon}_t^{ck}$	d_t
0.26	0	0
0.0026	0.00117	0.99

Table 9. Calibrated material properties for CPD model for strengthened masonry.

The plastic characteristics for the CDP model were kept constant in all cases and were taken from the recommendations given in Abaqus manual [12] and some modifications were performed according to the findings in the available literature [1, 10]. The constant coefficient (Kc) and the ratio of biaxial compressive yield strength to uniaxial compressive yield strength ($\sigma_{b0} / \sigma_{c0}$) are used to define the yield function of the model, the viscosity parameter (μ) affects the numerical stability of the constitutive law, the dilatation angle (ψ) is used to shape the potential flow and the eccentricity (ϵ) defines the rate at which the function approaches the asymptote [10, 12].

ψ	ϵ	$\sigma_{b0} / \sigma_{c0}$	K_c	μ
10	0.1	1.16	0.67	0.01

Table 10. Material properties for the plastic characteristics of CDP model.

6 INTERACTION PROPERTIES

In the simplified micro-modelling approach, interaction is used to define the properties of the mortar and possible cracks in the brick units, because it is not possible to simulate this effect with the concrete damaged plasticity model [1, 8, 9].

Cracks in the bricks were modelled only were expected to happen. For instance, the walls subjected to diagonal compression were expected to have shear failure in the mortar joints, so interaction properties for cracks in the bricks are not modelled because it would only complicate the model. On the other hand, the walls subjected to uniaxial compression exhibit cracks in both, the mortar and in the bricks, too. So, in those cases interaction properties for brick cracking were taken into account.

The interaction was modelled to exhibit normal, frictional and cohesive behaviour. Some of the input values for the interaction properties were taken from the experimental tests [2], while the others that cannot be obtained from the tests were calibrated from the FE analyses.

6.1 Normal behaviour

The distance that separates two surfaces is called clearance. When the clearance is zero, the surfaces are in contact and when the contact pressure between them becomes negative, they shall separate. This behaviour between two surfaces is called hard contact. When the surfaces are in contact, any pressure can be transferred between them, but it does not allow transmission of tension force through the contact [12], Figure 12.

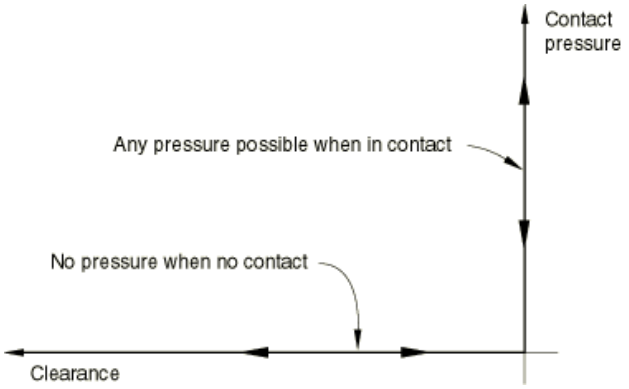

Figure 12. Contact pressure - clearance relationship [12].

6.2 Frictional behaviour

When two surfaces are not slipping one relative to another, there is friction in their contact. This friction depends of the contact pressure and the material properties of contact surfaces. The basic concept of the Coulomb friction model used to simulate this effect, is that two contacting surfaces can carry shear stress up to a certain value before they begin to slide relative to each other. This condition is known as sticking, and the maximum stress as critical shear stress, Figure 13.

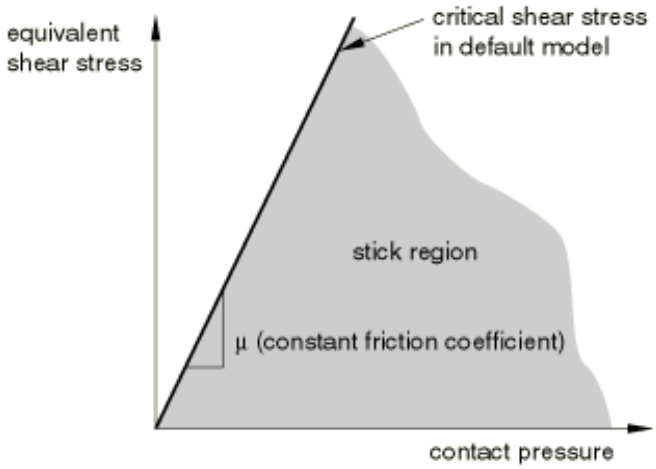

Figure 13. Coulomb friction model [12].

For defining the frictional behaviour with the Coulomb friction model, a constant isotropic friction coefficient (μ) was applied to the FE models, which directly affects the failure mechanism of the masonry. By increasing the friction coefficient, the ductility of the model increases and vice versa. Through calibration of the failure mechanisms, the most suitable value of the friction coefficient for both old, unreinforced and strengthened masonry was adopted as $\mu=0.45$.

6.3 Cohesive behaviour

Cohesive contact behaviour is primarily intended for situations where the bond thickness is negligible. Otherwise, it may be more appropriate to model the response using solid elements [12]. This behaviour is defined as a surface interaction property and is used to model bond separation or sticky contact through traction and separation, Figure 14.

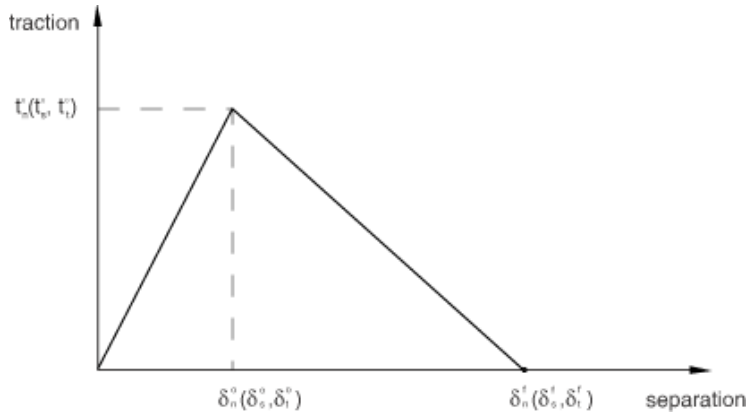

Figure 14. Cohesive behaviour defined by the traction - separation relationship with linear damage evolution.

Since cohesive parameters have no effect on the models exposed to uniaxial compression perpendicular to the interactions, the calibration of these parameters will depend purely on the models subjected to diagonal compression, i.e., W – DP and W – DP – RPP.

The stiffness coefficients (K) are the input parameters defining the cohesive behaviour in normal (K_{nn}), first (K_{ss}), and second (K_{tt}), shear direction. These coefficients represent the required traction to separate two surfaces and their values were taken according to Lourenco's recommendations [1] and through additional FE model calibration, Table 11.

Model	K_{nn} [N/mm^3]	K_{ss} [N/mm^3]	K_{tt} [N/mm^3]
Old Masonry	110	50	50
Strengthen Masonry	400	185	185
Cracks in the bricks	2000	925	925

Table 11. Cohesive, normal and shear stiffness parameters.

Damage of the contact occurs when the maximum stress (traction) in normal (t^o_n) and tangential direction (t^o_s, t^o_t) is surpassed. The input parameters were calibrated according to the shear strength of the contact, because that is the failure mechanism of the model subjected to diagonal compression. The normal stress was calculated as 1.4 times the calibrated shear stress, Table 12.

Model	t^o_n [MPa]	t^o_s [MPa]	t^o_t [MPa]
Old Masonry	0.055	0.075	0.075
Strengthen Masonry	0.200	0.280	0.280
Cracks in the bricks	1.000	1.400	1.400

Table 12. Peak values of the contact stress for purely separation in normal, first or second shear direction.

After the maximum stress is reached, linear softening of the contact begins until the maximum (total plastic) displacement, δ_m^{max}, is attained. At that point the separation of the contact occurs [12]. This maximum displacement in all analyses was taken as 1.5 mm and the value was obtained by FE model calibration.

7 VALIDATION OF RESULTS

The validation of the results was done by comparison of the force – displacement curves and the failure mechanisms calculated by the FE analysis and obtained from the experimental tests.

7.1 Comparison of force – displacement curves

The experimental test curve used in the comparison was an averaged curve from the three tested wallets for each of the four different tests. Figures 15-18 show a compassion of the force – displacement curves for uniaxial and diagonal compression cases calculated by FE analysis and obtained from the tests. In general, very good agreement between results was obtained.

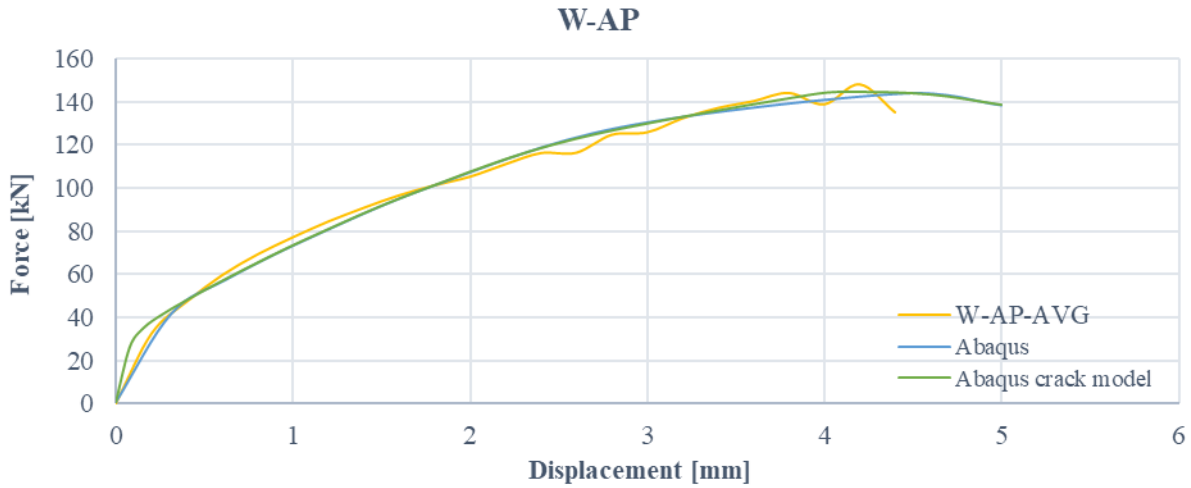

Figure 15. Force - displacement curves of old, unreinforced masonry subjected to uniaxial compression.

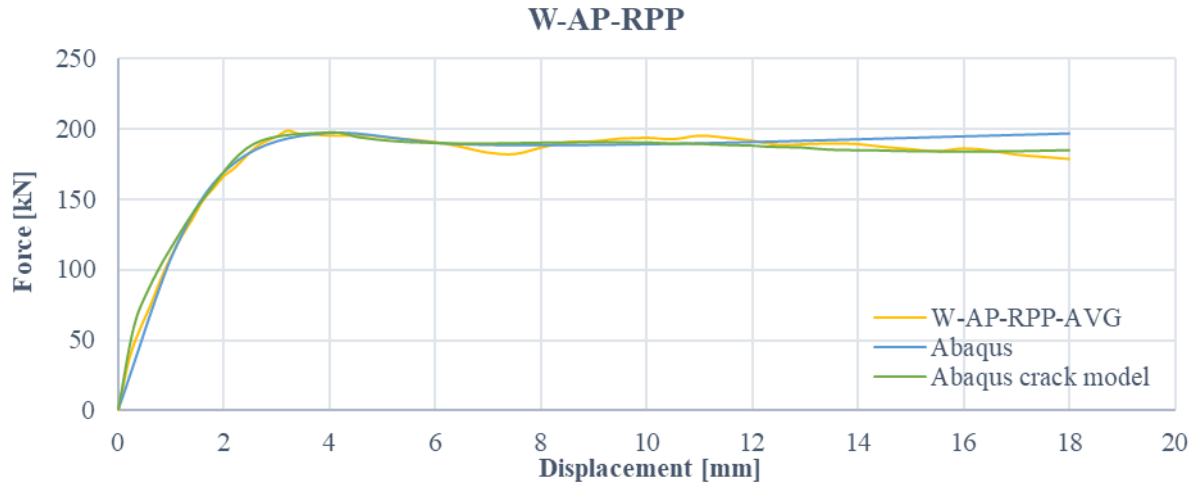

Figure 16. Force - displacement curves of strengthen masonry subjected to uniaxial compression.

Figures 15 and 16 show the results from uniaxial compression of old, unreinforced and strengthened masonry. The results from the experimental analysis and both models, with and without cracks are almost matching. The only benefit from the model with cracks in the bricks is the visualization of the crack development and their continuity throughout the model. Another thing worth noting is that the curves have similar maximal displacement. This proves that the combination of Kent and Park model with the Concrete damaged plasticity model provides an excellent prediction of the behaviour of masonry structures subjected to compression.

The FE models taking into account possible cracks in the bricks have higher stiffness in the elastic region, because of their higher values of traction than the yield strength of the masonry.

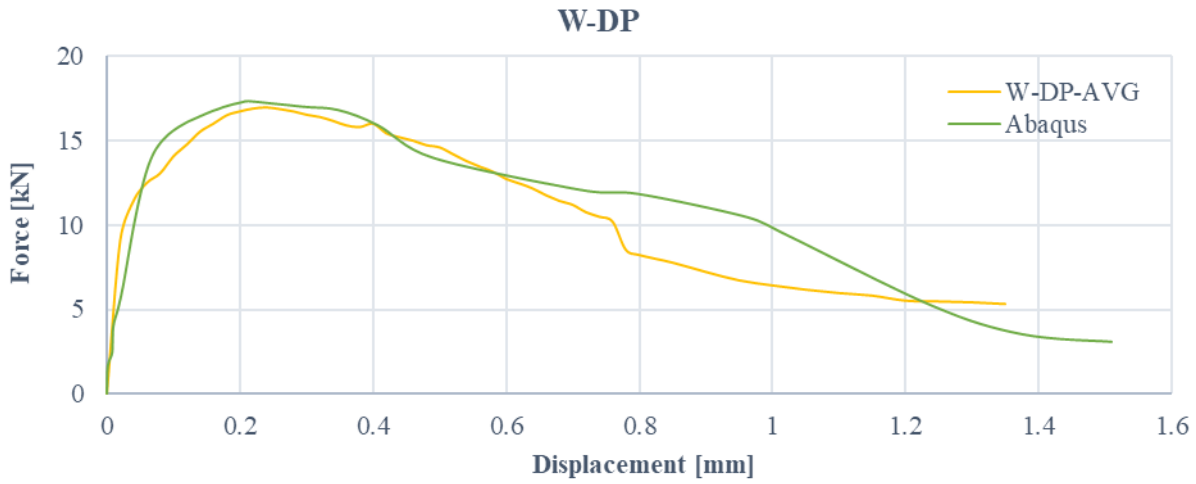

Figure 17. Force - displacement curves of old, unreinforced masonry subjected to diagonal compression.

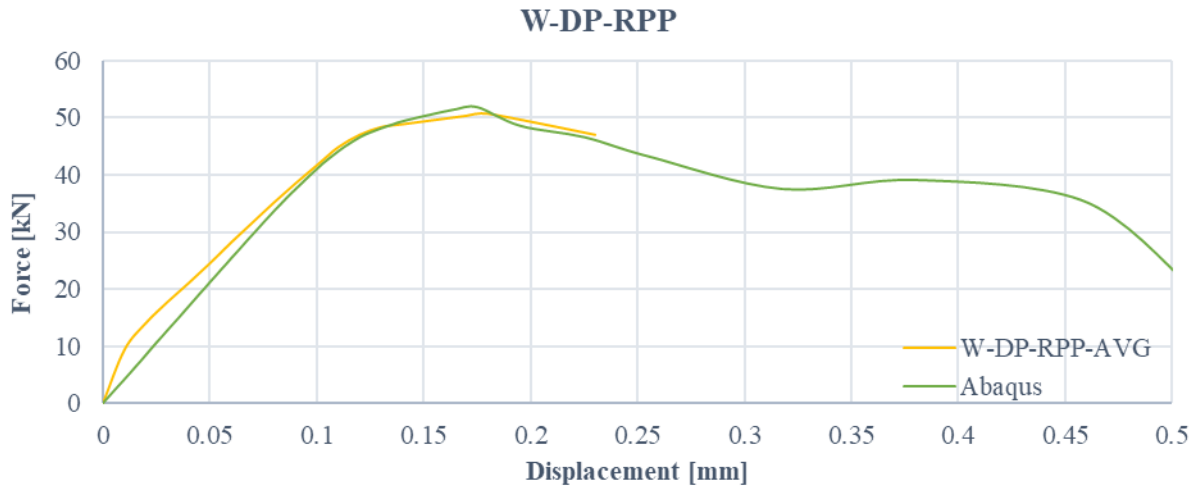

Figure 18. Force - displacement curves of strengthen masonry subjected to diagonal compression.

Figures 17 and 18 present the results calculated for the case of diagonal compression of old, unreinforced and strengthened masonry and their comparison with the test results. The calculated results are in line with the experimentally obtained results and the form of the calculated curves follow the ones obtained from the experimental tests. Moreover, both curves have similar maximal forces at similar displacement values. The unreinforced masonry subjected to diagonal compression presents similar maximal displacements as the ones in the tests. The strengthened masonry, as expected, shows similar displacements as the ones obtained with the

tests. The tests results presented in Figure 18 are prematurely terminated to protect the measurement equipment from damage during the execution of the tests.

7.2 Comparison of failure mechanisms

7.2.1. W – AP

The masonry wallets subjected to uniaxial compression exhibit sudden failure represented by brick and joint cracking. Almost no crushing of the bricks was obtained, see Figure 19. The formation of the cracks follows the maximum stresses in the interaction, and corresponds well to the experimental test, Figure 20. Also, as seen from Figure 20, there is discontinuity in the crack pattern, and the results are presented from the model without modelling possible cracks in the bricks.

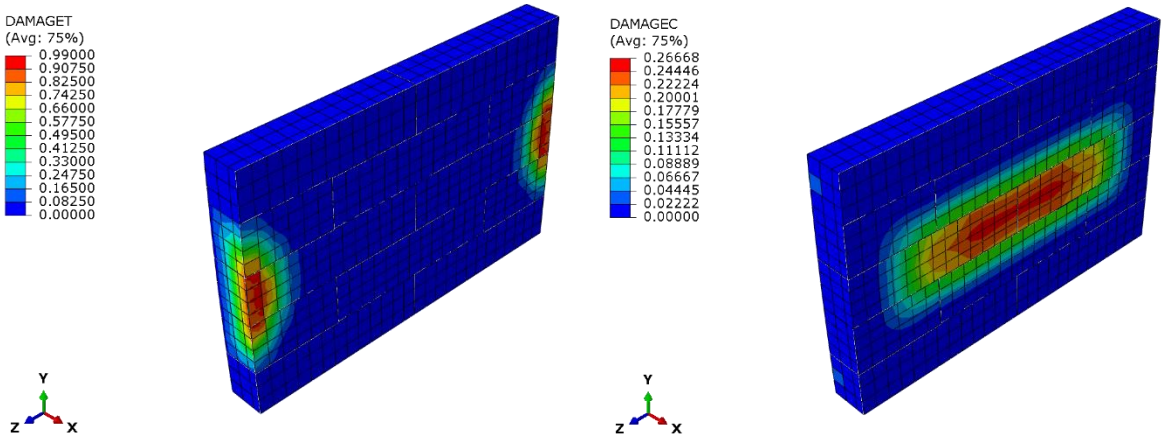

Figure 19. Damage in the W – AP model due to tension and compression.

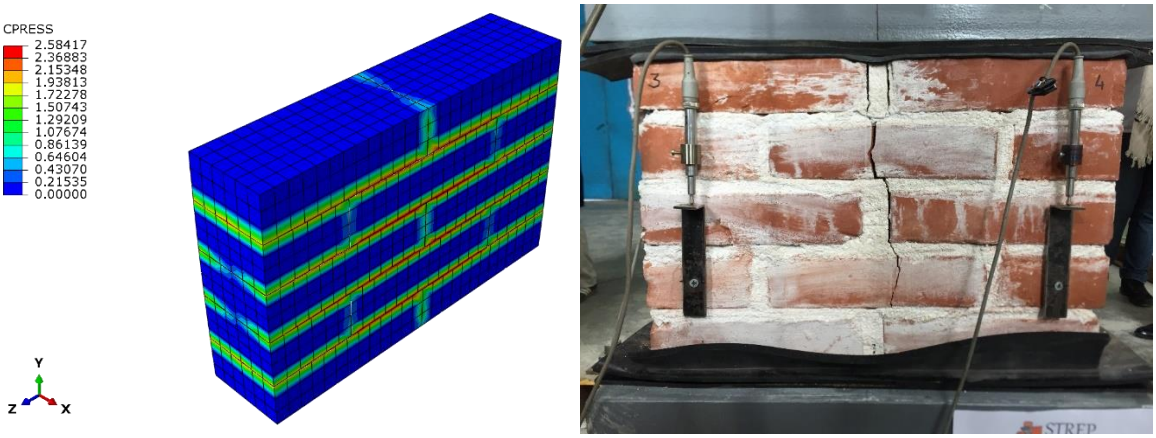

Figure 20. Damage comparison in the mortar in the W – AP model and experimental test.

7.2.2. W – AP – RPP

The strengthened masonry wallets subjected to uniaxial compression have visibly more ductile failure, which is evident from the crushing of the bricks in both experimental test and FE model.

These deformations are due to the development of plastic deformations in the bricks when exceeding their compressive strength. There is also a separation of part of the bricks and mortar on the sides of the walls. This separation occurs as a result of exceeding the tensile

strength of the bricks and the adhesion properties of the new to the old mortar, Figure 23. The same characteristics can also be observed in the FE analyses, which show the damage of the bricks in tension and pressure at failure, Figure 21, 22.

In Figure 22, the cracks in the mortar joints are visible throughout the whole masonry domain, owing to the fact that a model with potential cracks in the bricks was used. The mesh formed from the cracks in the FE model corresponds well to the one obtained from the experimental tests.

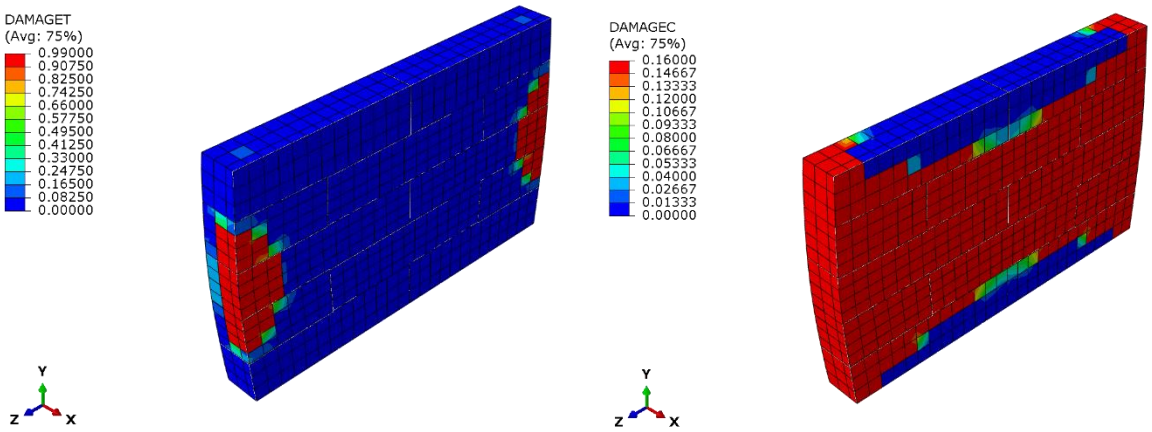

Figure 21. Damage in the W – AP – RPP model due to tension and compression.

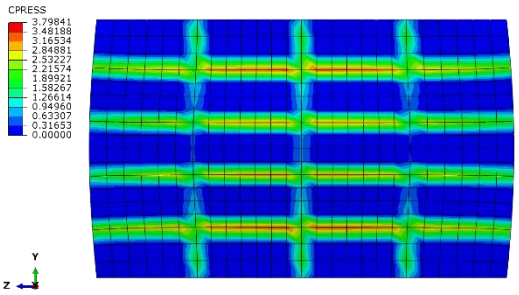

Figure 22. Damage in the mortar in the W – AP – RPP model.

Figure 23. Damage in the W – AP – RPP wallet from the experimental test.

7.2.3. W – DP

The masonry subjected to diagonal compression also exhibits brittle and sudden failure. There is almost no damage in the bricks, while the cracks develop in the joints until they slip completely. The angle of the crack development and brick compressive damage matches with the results obtained from the experimental tests, Figure 24, 25.

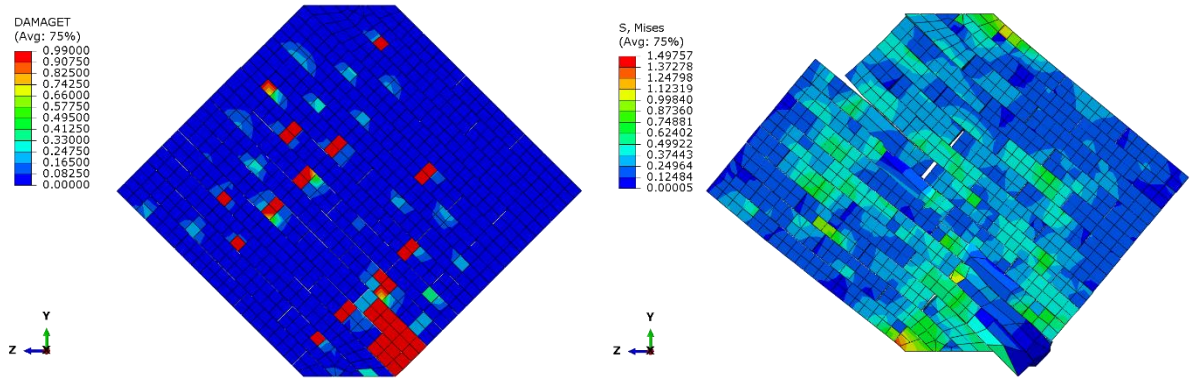

Figure 24. Damage in the bricks and in the mortar calculated with the W – DP model.

Figure 25. Typical damage of the W – DP wallets obtained from the experimental tests.

7.2.4. W – DP – RPP

In the strengthened masonry subjected to diagonal compression, the bricks experience more damage, which was noticeable even in the experimental tests and presented by crushing sounds while testing, Figure 26.

The experimental tests were loaded until the certain strength degradation and were not performed until complete failure of the wallets. Accordingly, the ultimate strains obtained from

the experimental test are essentially larger than those calculated with the FE models. Also, because of this effect, no fracture appears in the FE analysis, and the direction of the development of the main cracks can only be seen. The failure mechanism is represented by a combination of shear cracks along the horizontal (bed) joints and tension cracks in the diagonal direction, following stair-case pattern between head and bed joints. The simulated failure mechanism is in good agreement with the failure mechanism obtained from the experimental tests, Figure 27.

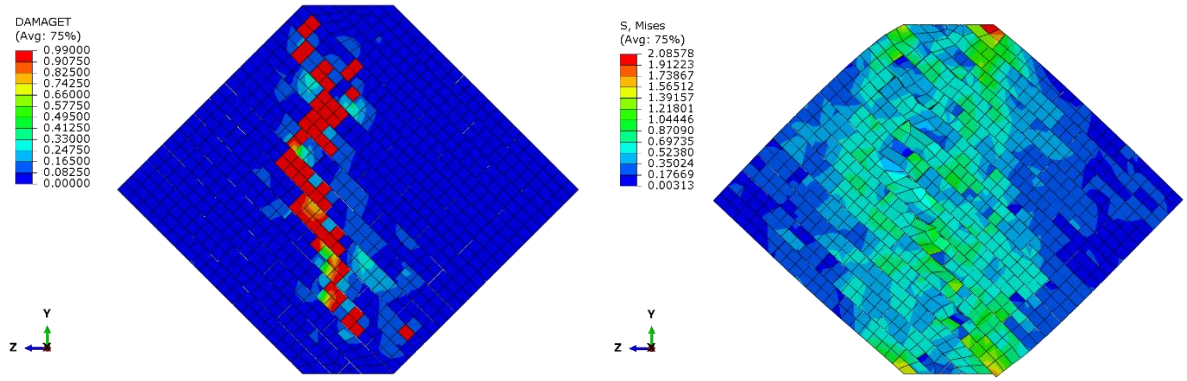

Figure 26. Damage in the bricks and in the mortar in the W – DP – RPP model.

Figure 27. Typical damage in the W – DP – RPP wallets obtained from the experimental tests.

8 CONCLUSIONS

This paper presents FE simulation of unreinforced and strengthened masonry and verification of the calculated results and failure mechanisms with experimental tests. Both, the unreinforced and strengthened masonry assemblages were subjected to uniaxial and diagonal compression.

Simplified micro-modelling proved to be the most efficient modelling strategy for masonry in terms of time demands and computational costs, without sacrificing the accuracy of the results. For these purposes, the brick units were smeared into one homogenous material represented by calibrated properties of the Concrete Damage Plasticity (CDP) model parameters. The impact of the mortar joints on the behaviour of masonry was considered through interface elements added between the brick units. The initiation of damage was considered based on the mortar strength and the damage evolution was defined as linear softening until the assigned plastic strains were reached.

From the finite element analysis, it was evident that even though different models were used, with different mortar properties subjected to different loading conditions, the calculated results in the simulations were in line with the experimental results. Aside from the force-displacement curves, the applied modelling approach was able to capture the realistic failure mechanism of the wall assemblages.

For uniaxial compression case, the Concrete Damage Plasticity model has the biggest impact on the results and the cohesive behaviour has no influence on it whatsoever. In this case, to properly simulate the failure mechanism, interface elements were needed to simulate not only the mortar, but also the cracks in the middle of the brick units. The interface elements that simulate potential cracks in the bricks have effect only for simulation of the failure mechanism, not on the force – displacement curves.

On the contrary, models subjected to diagonal compression, show that the Concrete damage plasticity model has small impact on the results, because the failure mostly occurs in the joints between the mortar and the brick units. In this case, the cohesive behaviour with damage initiation and damage evolution was the key element to properly simulate the tests. There is no need to model the potential cracks in bricks, if their strength is not extremely lower than the one of the mortar.

In conclusion, the results presented in this paper prove that masonry structures with different material characteristics exposed to complex stress states can be effectively simulated with simplified micro-modelling strategy and with the Concrete damage plasticity model and interface elements with normal, frictional and cohesive behaviour by calibrating the required parameters.

9 ACKNOWLEDGMENTS

This research is part of the scientific-research project "Strengthening of masonry with joint repointing (STREP)", led by Dumova-Jovanoska et al., University Ss. Cyril and Methodius in Skopje, Faculty of Civil Engineering - Skopje as the project coordinator [3]. The realization of this project was made possible with the cooperation of three partner institutions, Faculty of Civil Engineering - Skopje, chair of Theory of structures and computational analysis and Institute of Earthquake Engineering and Engineering Seismology, both part of the Ss. Cyril and Methodius University in Skopje, responsible for execution of the experimental tests and numerical simulations and the company ADING A.D. from Skopje, which made and produced the specially modified joint repointing material, as well as its application on the test models. The results, opinions and conclusions expressed in this paper are solely those of the authors and do not necessarily reflect those of the sponsoring institutions.

REFERENCES

[1] P.B. Lourenco, *Computational strategies for masonry structures*. PhD thesis, Faculty of civil engineering, Delft University of Technology, Delft. Netherlands, 1996.

[2] M. Gosheva, *Experimental and numerical analysis of the behavior of unstrengthened and strengthened masonry with repointing mortar and polypropylene straps*. Master thesis, Ss. Cyril and Methodius University in Skopje, Faculty of Civil Engineering – Skopje, N. Macedonia, 2021.

[3] E. Dumova-Jovanoska. S. Churilov. V. Shendova. L. Kristevska, Report from the research project "Masonry strengthening by joint repointing - STREP". Ss. Cyril and Methodius University in Skopje, Faculty of Civil Engineering – Skopje, Institute of Earthquake Engineering and Engineering Seismology and ADING A.D., Skopje, 2021.

[4] B. Damchevski. S. Churilov. E. Dumova-Jovanoska, Mechanical characterisation of polymer fibre-reinforced cement-based mortar for masonry joint repointing. *16th European Conference on Earthquake Engineering*, Thessaloniki, Greece, June 18-21, 2018.

[5] M. Tomaževic, *Earthquake – resistant design of masonry buildings*, *Series on Innovation in Structures and Construction: Vol.* 1. Imperial College Press, London, England, 1999.

[6] MKC EN 1052-1:200, *Methods of test for masonry. Determination of compressive strength*. ISRM. Skopje, N. Macedonia, 2009.

[7] ASTM E519-02, *Standard Test Method for Diagonal Tension (Shear) in Masonry Assemblages*. ASTM International, West Conshohocken, PA, 2002.

[8] A.J. Aref, K.M. Dolatshahi, A three-dimensional cyclic meso-scale numerical procedure for simulation of unreinforced masonry. *Computers and Structures*. **120**, 9-23, 2013.

[9] M. Bolhassani, A.A. Hamid, A.C.W. Lau, F. Moon, Simplified micro modeling of partially grouted masonry assemblages. *Construction and Building Materials,* **83**, 159-173, 2015.

[10] M. Resta, A. Fiore, P. Monaco, Non-Linear Finite Element Analysis of Masonry Towers by adopting the Damage Plasticity Constitutive Model. *Advances in Structural Engineering*, **16**, 791-803, 2013.

[11] A.H. Chopra, *Dynamics of Structures, Theory and Aplications to Earthquake Engineering.* Prentice Hall, Englewood Cliffs, New Jersey, USA, 1995.

[12] Abaqus Analysis User's Guide, *Abaqus 6.14*. Simulia, Dassault Systems Corporation, Providence, RI, USA.

[13] J. Lubliner, J. Oliver, S. Oller, E. Oñate, A plastic-damage model for concrete. *International Journal of Solids and Structures*, **25**, 299–326, 1989.

[14] J. Lee, G. L. Fenves, Plastic-damage model for cyclic loading of concrete structures. *Journal of Engineering Mechanics*, **124**, 892–900, 1998.

[15] D.C. Kent, R. Park, Flexural members with confined concrete. *Journal of the Structural Division*, **97**, 1969 – 1990, 1971.